

CARLO GAVAZZI

CARLO GAVAZZI SPACE SpA

ACOP

Doc. Type: <b>REPORT</b>		DRD N°: E18	
Doc. N°: <b>ACP-RP-CGS-006</b>	Issue: <b>1</b>	Date: <b>Jan. 2005</b>	Page <b>1</b> Of <b>30</b>
Title : <b>THERMAL ANALYSIS AND DESIGN REPORT</b>			

	Name & Function	Signature	Date	DISTRIBUTION LIST		
				N	A	I
Prepared by:	ACOP Team	<i>[Signature]</i>	21/1/05	Internal		
Approved by:	M. Grilli (IU/SE)	<i>[Signature]</i>	21/1/05			
	G. Magistrati (IU/SE)	<i>[Signature]</i>	21/1/05			
	D. Laplena (PA/SF)	<i>[Signature]</i>	21/01/05			
	*C. Cinquepalmi (PA/CC)	<i>[Signature]</i>	21/01/05			
	M. Molina (DT/MT)	<i>[Signature]</i>	21/1/05			
Application authorized by:	C. Pini (IU/PM)	<i>[Signature]</i>	21.1.05	External M. Conte (ASI)		
Customer / Higher Level Contractor						
Accepted by:						
Approved by:						

N=Number of copy A=Application I=Information


Data Management:

*[Signature]*

Date

21-5-05

File: ACP-RP-CGS-006\_issue\_1.doc

 CARLO GAVAZZI SPACE SpA	<b>ACOP</b>	Doc N°: <b>ACP-RP-CGS-006</b>
	THERMAL ANALYSIS AND DESIGN REPORT	Issue : <b>1</b> Date: <b>Jan. 2005</b> Page <b>2</b> of <b>30</b>

CHANGE RECORD			
ISSUE	DATE	CHANGE AUTHORITY	REASON FOR CHANGE AND AFFECTED SECTIONS
1	Jan. 2005		First issue



## THERMAL ANALYSIS AND DESIGN REPORT


*Doc*  
*N°:* **ACP-RP-CGS-006**

*Issue* **1** *Date:* **Jan. 2005**

*Page* **3** *of* **30**

## LIST OF VALID PAGES

[illegible]

 CARLO GAVAZZI SPACE SpA	<h1>ACOP</h1>		Doc N°: <b>ACP-RP-CGS-006</b>
	THERMAL ANALYSIS AND DESIGN REPORT		Issue : <b>1</b> Date: <b>Jan. 2005</b>
		Page <b>4</b> of <b>30</b>	

## TABLE OF CONTENT


<b>1. SCOPE OF THE DOCUMENT .....</b>	<b>5</b>
<b>2. DOCUMENTS .....</b>	<b>6</b>
2.1 APPLICABLE DOCUMENTS .....	6
2.2 REFERENCE DOCUMENTS .....	7
<b>3. SYSTEM DESCRIPTION.....</b>	<b>8</b>
<b>4. THERMAL CONTROL CONCEPT AND THERMAL DESIGN DESCRIPTION .....</b>	<b>11</b>
<b>5. THERMAL REQUIREMENTS .....</b>	<b>12</b>
5.1 BOUNDARY TEMPERATURES AND THERMAL INTERFACES .....	13
<b>6. THERMAL LOADS .....</b>	<b>14</b>
<b>7. MODEL DESCRIPTION AND THERMAL ANALYSIS .....</b>	<b>17</b>
7.1 THERMAL AND FLUIDIC MODEL DESCRIPTION.....	17
7.1.1 INLET AND OUTLET DUCTS, FRONT PANEL.....	17
7.1.2 FINNED CHANNELS.....	18
7.2 THERMAL CASES.....	18
<b>8. ANALYSIS RESULTS .....</b>	<b>20</b>
8.1 PRESSURE LOSS.....	28
<b>9. CONCLUSIONS.....</b>	<b>30</b>

## LIST OF FIGURES

<i>Figure 1: Sketch of the mechanical design of ACOP .....</i>	<i>8</i>
<i>Figure 2: Flow direction of the supplied cooling air .....</i>	<i>10</i>
<i>Figure 3: The allocation of ACOP thermal load for case 1 and the sketch of the heat transfer direction (HDD 1 and 3 are operating).....</i>	<i>14</i>
<i>Figure 4: The allocation of ACOP thermal load for case 2 and the sketch of the heat transfer direction (HDD 1 and 2 are operating).....</i>	<i>14</i>
<i>Figure 5: ACOP lumped parameter model to calculate heat distribution (PL and PR).....</i>	<i>15</i>
<i>Figure 6: The allocation of ACOP thermal load for case 3 and the sketch of the heat transfer direction... </i>	<i>16</i>
<i>Figure 7: Predicted velocity along the middle cross section of ACOP with a flow rate of 12 cfm .....</i>	<i>20</i>
<i>Figure 8: Predicted heat transfer coefficient in the fin channels via the laminar flow model .....</i>	<i>21</i>
<i>Figure 9: Predicted temperature profile of the fin channels and chassis for case 1 .....</i>	<i>22</i>
<i>Figure 10: Predicted temperature profile of the front panel for case 1 .....</i>	<i>23</i>
<i>Figure 11: Predicted temperature profile of the cooling air for case 1.....</i>	<i>24</i>
<i>Figure 12: Predicted temperature profile of the cooling air at the central section of ACOP for case 1 .....</i>	<i>25</i>
<i>Figure 13: Temperature profile of air in the fin channels at the central cross section for case 1 .....</i>	<i>25</i>
<i>Figure 14: Predicted temperature profile of the fin channels and chassis for case 2.....</i>	<i>26</i>
<i>Figure 15: Predicted temperature profile of the fin channels and chassis for case 3.....</i>	<i>27</i>


## LIST OF TABLES

<i>Table 1: Geometry of the fin channels of ACOP and the applied heat transfer coefficient h .....</i>	<i>9</i>
<i>Table 2: ACOP flight model typical power budget and requirements .....</i>	<i>12</i>
<i>Table 3: Inlet cooling air conditions and front-panel convection coefficient .....</i>	<i>16</i>
<i>Table 4: Predicted maximum Temperature for the analysed cases .....</i>	<i>19</i>
<i>Table 5: Fin channel pressure loss of one side with different flow rates and pressures of cooling air.....</i>	<i>29</i>

 CARLO GAVAZZI SPACE SpA	<h1>ACOP</h1>	<i>Doc N°:</i> <b>ACP-RP-CGS-006</b>
	THERMAL ANALYSIS AND DESIGN REPORT	<i>Issue :</i> <b>1</b> <i>Date:</i> <b>Jan. 2005</b> <i>Page</i> <b>5</b> <i>of</i> <b>30</b>

## 1. SCOPE OF THE DOCUMENT


This report initially describes the mechanical design for the purpose of accomplishing the thermal management design method in order to meet the temperature requirements of the ACOP printed circuit boards and the main parts (Hard Disks). The constraints required by the ISS cabin are also documented. The methodology of the thermal and fluidic analysis is described in more details. The predicted results show the compliance of the thermal design to the requirements. Discussions of the calculated results is also described.

 CARLO GAVAZZI SPACE SpA	<h1>ACOP</h1>		Doc N°: <b>ACP-RP-CGS-006</b> Issue : <b>1</b> Date: <b>Jan. 2005</b> Page <b>6</b> of <b>30</b>
	THERMAL ANALYSIS AND DESIGN REPORT		

## 2. DOCUMENTS

### 2.1 APPLICABLE DOCUMENTS

AD	Doc. Number	Issue / Date	Rev.	Title / Applicability
1	SSP 52000-IDD-ERP	D / 6/08/03		EXpedite the PROcessing of Experiments to Space Station (EXPRESS) Rack Payloads Interface Definition Document
2	NSTS/ISS 13830	C / 01/12/1996		Implementation Procedures for Payloads System Safety Requirements – For Payloads Using the STS & ISS.
3	JSC 26493	17/02/1995		Guidelines for the preparation of payload flight safety data packages and hazard reports.
4	SSP 50004	April 1994		Ground Support Equipment Design requirements
5	SSP-52000-PDS	March 1999	B	Payload Data Set Blank Book
6	SSP 52000-EIA-ERP	Feb. 2001	A	Express Rack Integration Agreement blank book for Express Rack payload
7	GD-PL-CGS-001	3 / 17/03/99		PRODUCT ASSURANCE & RAMS PLAN
8	SSP 52000 PAH ERP	Nov. 1997		Payload Accommodation Handbook for EXPRESS Rack
9	SSP 50184	D / Feb. 1996		Physical Media, Physical Signaling & link-level Protocol Specification for ensuring Interoperability of High Rate Data Link Stations on the International Space Program
10	SSP 52050	D / 08/06/01		S/W Interface Control Document for ISPR ***ONLY FOR HRDL, SECTION 3.4 ***
11	ECSS-E-40	A / April 1999	13	Software Engineering Standard
12	AMS02-CAT-ICD-R04	29/08/2003	04	AMS02 Command and Telemetry Interface Control document. Section AMS-ACOP Interfaces
13	SSP 52000-PVP-ERP	Sept. 18, 2002	D	Generic Payload Verification Plan EXpedite the PROcessing of Experiments to Space Station (EXPRESS) Rack Payloads
14	NSTS 1700.7B	Rev. B Change Packet 8 / 22.08.00		Safety Policy and Requirements for Payloads using the STS
15	NSTS 1700.7B Addendum	Rev. B Change Packet 1 01.09.00		Safety Policy and Requirements for Payloads using the International Space Station
16	SSP 52005	Dec. 10, 1998		Payload Flight equipment requirements and guidelines for safety critical structures
17	NSTS 18798B	Change Packet 7 10.00		Interpretation of NSTS Payload Safety Requirements
18	MSFC-HDBK-527	15/11/86	E	Materials selection list for space hardware systems Materials selection list data
19	GD-PL-CGS-002	1/ 12-02-99		CADM Plan
20	GD-PL-CGS-004	2/07-04-03		SW Product Assurance Plan
21	GD-PL-CGS-005	2/09-05-03		SW CADM Plan

 CARLO GAVAZZI SPACE SpA	<h1>ACOP</h1>		Doc N°: <b>ACP-RP-CGS-006</b> Issue : <b>1</b> Date: <b>Jan. 2005</b> Page <b>7</b> of <b>30</b>
	THERMAL ANALYSIS AND DESIGN REPORT		

## 2.2 REFERENCE DOCUMENTS

RD	Doc. Number	Issue / Date	Rev.	Title
1	GPQ-MAN-02	1		Commercial, Aviation and Military (CAM) Equipment Evaluation Guidelines for ISS Payloads Use
2	BSSC (96)2	1 / May 96		Guide to applying the ESA software engineering standards to small software projects
3	GPQ-MAN-01	2 / Dec. 98		Documentation Standard for ESA Microgravity Projects
4	MS-ESA-RQ-108	1 / 28-Sep-2000		Documentation Requirements For Small And Medium Sized MSM Projects
5	PSS-05			Software Engineering Standards
6	GPQ-010	1 / May 95	A	Product Assurance Requirements for ESA Microgravity Payload. Including CN 01.
7	GPQ-010-PSA-101	1		Safety and Material Requirements for ESA Microgravity Payloads
8	GPQ-010-PSA-102	1		Reliability and Maintainability for ESA Microgravity Facilities (ISSA). Including CN 01
9	ISBN 0-9638178-4-1	1999		I-DEAS 8 Course Guide
10	Int. J. Heat Mass Transfer, V.24, No. 9	1981		Temperature and Concentration Profiles in Fully Turbulent Boundary Layers
11	Frank P. Incropera, and David P. DeWitt, John Wiley & Sons.	2002		Introduction to Heat Transfer
12	CSIST Report	2004		Temperature Measurement of ACOP Hard Disk Driver
13	Transactions of the ASME, Vol.77	Nov., 1955		Numerical Solutions for Laminar-flow heat Transfer in Circular Tubes
14	Mechanical Eng. Dep., University of Kansas, Lawrence	July, 1982		Convective Heat Transfer

### 3. SYSTEM DESCRIPTION

Figure 1 shows the back view and the side view of ACOP.

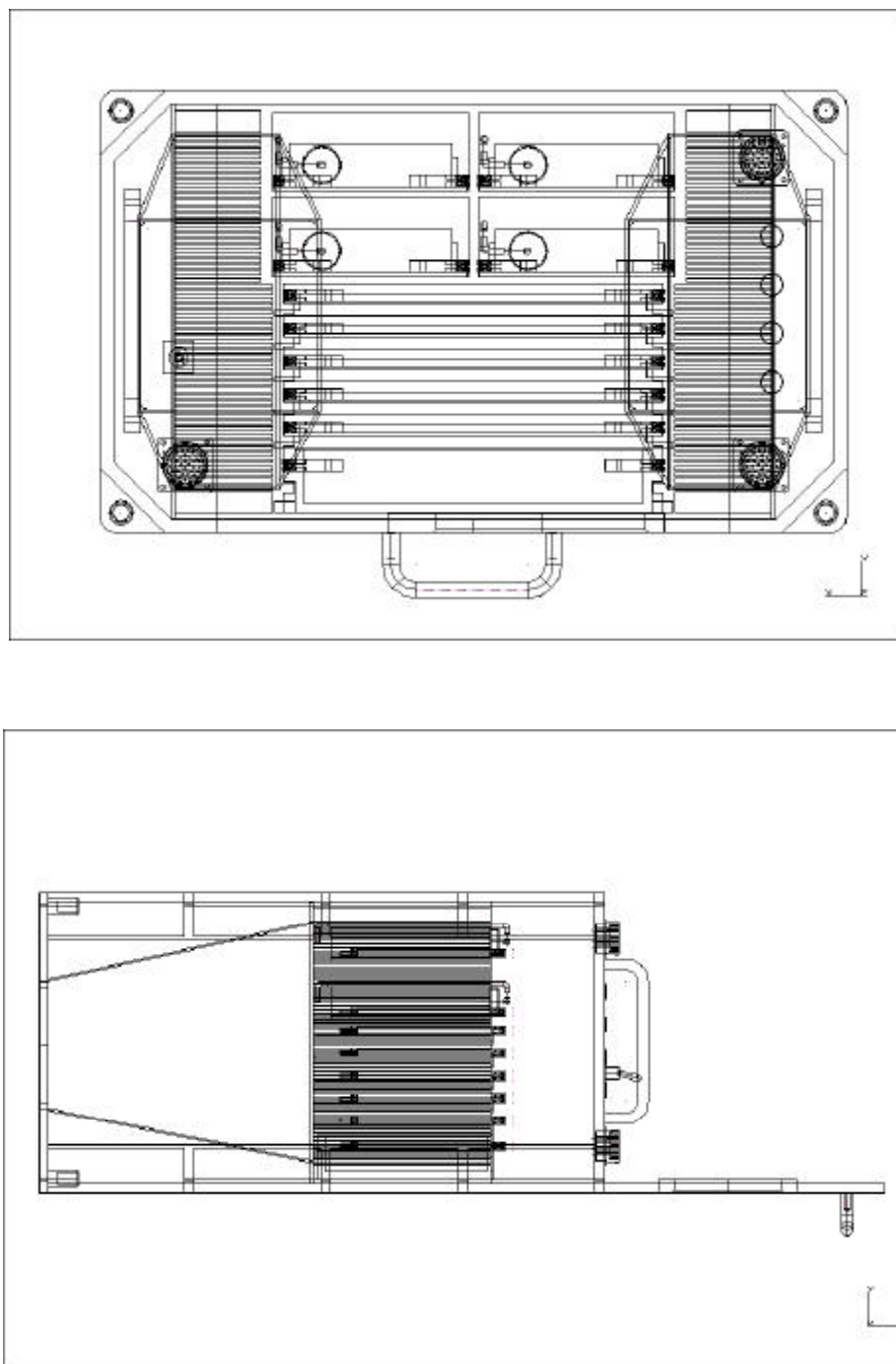



Figure 1: Sketch of the mechanical design of ACOP

 CARLO GAVAZZI SPACE SpA	<h1>ACOP</h1>		Doc N°: <b>ACP-RP-CGS-006</b>
	THERMAL ANALYSIS AND DESIGN REPORT		Issue : <b>1</b> Date: <b>Jan. 2005</b> Page <b>9</b> of <b>30</b>

The “EXPRESS Rack” provides ACOP with the cooling air through ducted ports at the back plate of ACOP. The width and height of the two square ports of the inlet and the outlet for the ducted cooling air are 110 mm X 110 mm each one. The ports are fitted with screens, with an open area ratio of 60.02%, in order to filter the cooling air. A typical flow rate, 15+/-3 cubic feet per minute (cfm), of the cooling air with a normal operation pressure of 10.2 lb/in<sup>2</sup> (psia) is blown into the inlet of ACOP as described in the applicable reference [1].

On ACOP side Two ducts are designed to connect the inlet and outlet ports with the fin channels as heat sinks extruded from the chassis of ACOP electronic modules in order to reduce the pressure loss. In case no duct is designed-in an abrupt expansion and contraction of the air flow would occur.

At both sides of the ACOP chassis, 56 fins are extruded respectively to be the heat sinks in order to increase both of the heat transfer area and the heat transfer coefficient of the cooling air. The thickness of the aluminium alloy fins is 1.5 mm with height and length of 60 mm and 162 mm respectively. The gap between two adjacent fins is 2.5 mm. See *Table 1*.

Number of fins at one side	Thickness	Height	Length
56	1.5 mm	60 mm	162 mm
Distance between two adjacent fins	Value of h by a semi-empirical correlation	Value of h by the CFD laminar flow model	Material
2.5 mm	40.3 W/m <sup>2</sup> °C	42.1 W/m <sup>2</sup> °C	7075-T7351

*Table 1: Geometry of the fin channels of ACOP and the applied heat transfer coefficient h*


The effective hydraulic diameter of the fin channels is calculated to be 4.8 mm. Under this value of the effective channel diameter, the thickness of the thermal boundary layer of the fin wall can be reduced to be a small value such that for a constant Nusselt number of a laminar channel flow, the heat transfer coefficient h, inverse to the effective diameter, can be enlarged to a desired value around 40 W/ m<sup>2</sup>°C. In addition to the increased heat transfer coefficient, the area for heat convection to the cooling air is also augmented significantly to decrease the thermal resistance, leading to an decrease of both of the boards and the parts working temperature.

The power dissipation is produced by every active part of each board in the ACOP electronic modules, including the four hard disk drivers. The power consumption in the form of heat conducts to the mounting board via the solder leads and the part case. The heat spreads to the board edge mainly via the copper layers implemented as the power and ground planes. Then, through the card-locker and the spacer fastening the boards to the inner side of the chassis, the heat conducts to the chassis. The fin channels extruded from the chassis absorb the heat to the surfaces. Finally the cooling air conveys away the heat via the forced convection.

Cooling air (see *Figure 2*) comes into the inlet, and passes through the filtering screen, and then is confined in and flows through the duct, and enters into the fin channels to take away the power, and comes out to the front chamber to cool the LCD panel, and then goes through the fin channels of the opposite side, and enters into the opposite duct and finally goes out to the Rack via the outlet port.

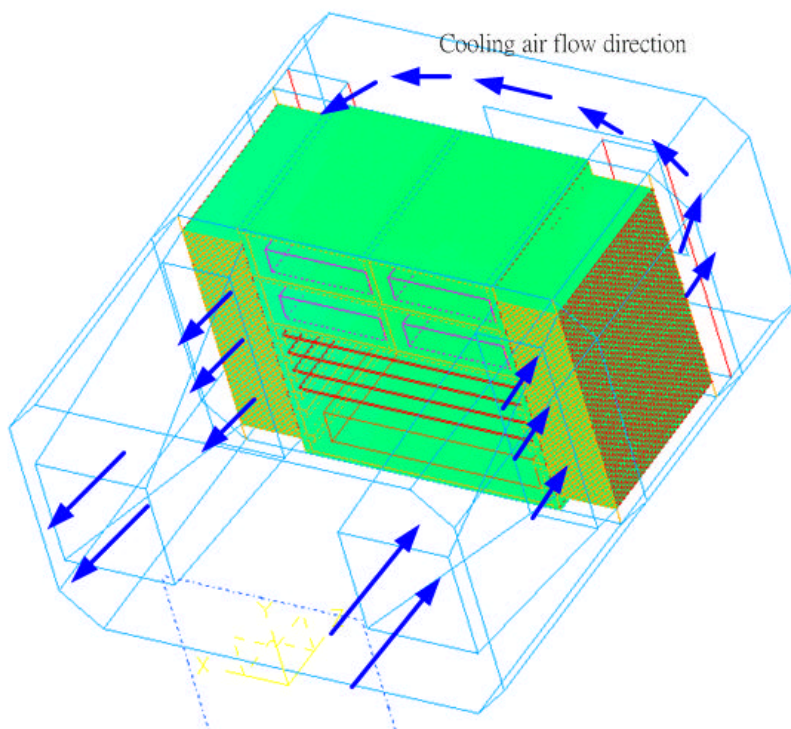



*Figure 2: Flow direction of the supplied cooling air*

 CARLO GAVAZZI SPACE SpA	<h1>ACOP</h1>		Doc N°: <b>ACP-RP-CGS-006</b>
	THERMAL ANALYSIS AND DESIGN REPORT		Issue : <b>1</b> Date: <b>Jan. 2005</b> Page <b>11</b> of <b>30</b>

## 4. THERMAL CONTROL CONCEPT AND THERMAL DESIGN DESCRIPTION

In ACOP, there are three main subsystems that consume power.

1. Four hard disk drivers, installed in the ACOP top chassis, are used to record the data collected by AMS-02. The drivers use spreaders to conduct the heat to the HDD edge. The commercial hard disk driver has a control board and a driver. Both of them will consume power. The power dissipation of parts on the controlled boards is nearly conducted through the copper layers of power planes and of ground planes to the board edge via the spacer, fixed to the chassis by a card-locker, to the chassis and spreads to the fins, and finally transfers to the cooling air.
2. Electronic boards: One single board computer, one “Compact-PCI 6U SATA & Ethernet” board, one “Compact-PCI 6U Video, USB and DIO board” board, one “Compact-PCI 6U HRDL” board and one “Power Distribution” board consisted of the controlling module of ACOP, are arranged in the down side of the ACOP chassis.
3. One LCD monitor is arranged on the front panel of ACOP to show the required information. (TBC).


 CARLO GAVAZZI SPACE SpA	<h1>ACOP</h1>			Doc N°:	ACP-RP-CGS-006	
				Issue : 1	Date:	Jan. 2005
THERMAL ANALYSIS AND DESIGN REPORT			Page	12	of	30

## 5. THERMAL REQUIREMENTS

The temperature requirements of the “Compact-PCI 6U SATA ” board and the HDD’s board is assumed to be 70 °C. The allowable working temperature of the LCD monitor is to be determined but we don’t expect serious issues, there. Via a thermal test of the Seagate HDD under operational mode, the measured temperature of the case is 70 °C . After the test the HDD still works normally. Thus, the maximum temperature for the HDD’s can be set for the time being to be 70 °C, with possible extensions after following measurement campaign (see the reference document [12]). The temperature requirement of the remaining boards is assumed to be 85 °C. However, for a larger ACOP reliability, the actual working temperature of its boards will be kept far below the requirements listed in Table 2.

LOC	Part Number	State	Type	Description	Power (W)	Temperature Requirements (° C)
Compact-PCI chassis						
SLOT1	ACOP-SBC	ON	Elec.	Single Board Computer	9.90	85
SLOT2	ACOP-T101	ON	Elec.	Compact-PCI 6U HRDL	1.65	70
SLOT3	ACOP-T102	ON	Elec.	Compact-PCI 6U Video + USB + DIO	1.65	85
SLOT4	ACOP-T103	ON	Elec.	Compact-PCI 6U Ethernet + SATA	5.0	85
SLOT5			Elec.	Spare	0.00	
Backplane	ACOP-BP	Passive	Elec.	Compact-PCI Backplane	0.00	
Power	ACOP-PS	ON	Elec.	Power Distribution	11.35	85
LCD						
Front Panel	ACOP-LCD	ON	Elec.	LCD Monitor	6.30	TBD
Hard Drives						
HDD LOC 1	TBD	ON	Elec.	Hot Plug SATA 250G HDD	12.54 **	70°C (TBC)
HDD LOC 2	TBD	ON	Elec.		12.54 **	70°C (TBC)
HDD LOC 3	TBD	Standby	Elec.		0.72	70°C (TBC)
HDD LOC 4	TBD	Standby	Elec.		0.72	70°C (TBC)
	HDD-CADDY		Mech.	Hard Drive caddy x 4	0.00	
Backplane	HDD-BP	Passive	Elec.	HDD Backplane	0.00	
Front Panel						
	ACOP-FPL		Mech.	Front Panel	0.0	49 *
Total					62.37	
<b>Notes:</b> * = For the crews to touch ** = Peak value considered for a conservative analysis						

Table 2: ACOP flight model typical power budget and requirements

 CARLO GAVAZZI SPACE SpA	<h1>ACOP</h1>		Doc N°: <b>ACP-RP-CGS-006</b>
	THERMAL ANALYSIS AND DESIGN REPORT		Issue : <b>1</b> Date: <b>Jan. 2005</b>
		Page <b>13</b> of <b>30</b>	

According to the thermal design of similar applications, 50 °C is the maximum wall temperature at which the working temperature of every board and of every component mounted on the board is still within the specification of the relevant data sheet.

## 5.1 BOUNDARY TEMPERATURES AND THERMAL INTERFACES

The cooling air temperature supplied by the AAA will be in the range from 18.3 to 29.4 °C, indicated in 5.3.1.3.2 of the applicable reference [1]. Here the cooling air temperature is assumed to be 30 °C for a conservative calculation of the model. The back-plate, top-plate, two side-plates, and bottom-plate of ACOP are assumed to be insulated from the outside environment.

The side plate to enclose the fin channels, in order to confine and to conduct the cooling passing through the extruded fins, is also considered to be insulated from the outside surrounding air, which exists between the ACOP outer enclosure and the ACOP modules. Only the front-panel, seeing the inner space of the ISS cabin, has a convection with the cabin by a heat transfer coefficient of 0.965 W/m<sup>2</sup> °C, as per 5.3.1.1.3 of the applicable document [1]. This value is utilized in the prediction model. The ISS cabin air temperature is assumed to be 30 °C.

For a conservative evaluation of the front panel (touch) temperature the thermal radiation effect is excluded in the model

## 6. THERMAL LOADS

Table 2 lists the power dissipation of boards and HDD's of ACOP. The total typical power dissipation of ACOP is estimated to be 62.37 W.

For the boards, the power dissipation is divided evenly between inlet and outlet duct and is uniformly allocated on the mounting slots to be the thermal load in the model. For the HDD's, the power dissipation is also divided evenly to load on the mounting slots of the chassis uniformly as shown in *Figures 3 and 4*. The power consumption of the LCD monitor is uniformly allocated on the fixed square panel of 170.5 by 126.5 mm.

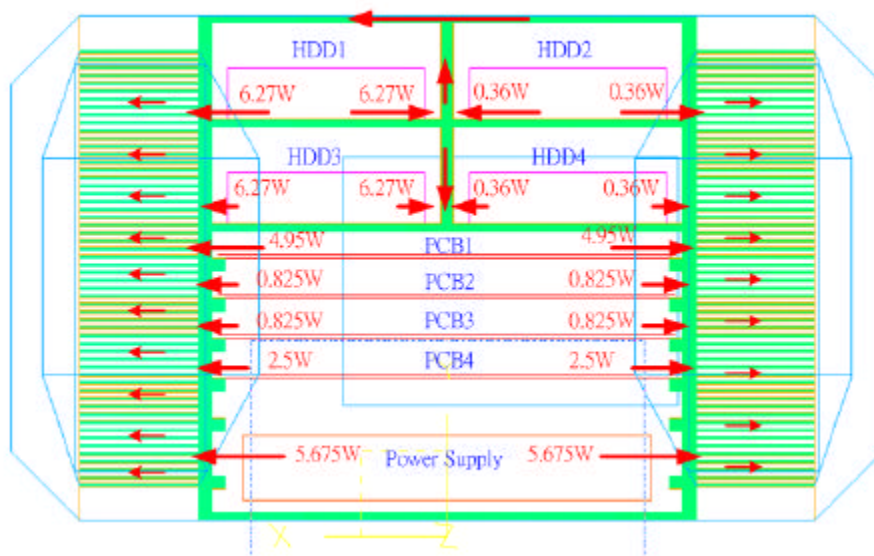


Figure 3: The allocation of ACOP thermal load for case 1 and the sketch of the heat transfer direction (HDD 1 and 3 are operating).

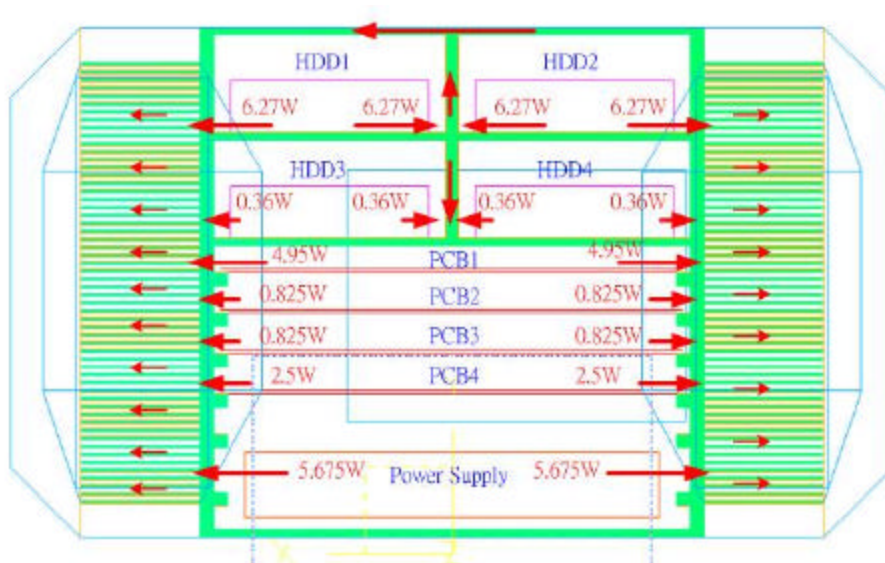



Figure 4: The allocation of ACOP thermal load for case 2 and the sketch of the heat transfer direction (HDD 1 and 2 are operating).

 CARLO GAVAZZI SPACE SpA	<h1 style="text-align: center;">ACOP</h1>	Doc N°: <b>ACP-RP-CGS-006</b> Issue : <b>1</b> Date: <b>Jan. 2005</b> Page <b>15</b> of <b>30</b>
	THERMAL ANALYSIS AND DESIGN REPORT	

Since the cooling air is supplied to the ACOP enclosure and cannot enter into the ACOP chassis, the power dissipation of parts spreads to the chassis slots mainly via board conduction, and slightly via thermal radiation. Thus, the total power dissipation can be allocated on the slots with a reasonable assumption. However, the actual power dissipation sharing between the two sides of the chassis is larger at the inlet side of the fin channels due to a low cooling air temperature. This effect is counterbalanced by transverse conduction of the outer chassis. According to the calculations of energy balance equations in algebraic form under the assumptions of lump systems for the fin channels the cooling air and the chassis (as shown in *Figure 5*), a more realistic power distribution between the air inlet and the air outlet is obtained

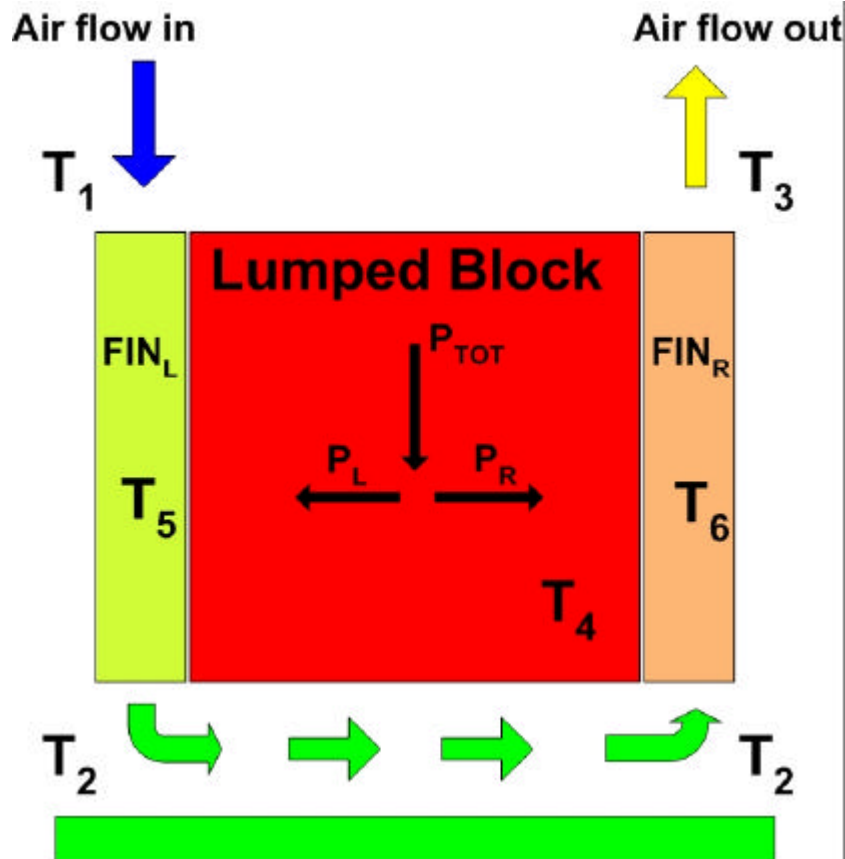


Figure 5: ACOP lumped parameter model to calculate heat distribution ( $P_L$  and  $P_R$ )

Governing equations are:

$$\begin{aligned}
 P_{TOT} &= P_L + P_R \\
 P_L &= k_{cont} (T_4 - T_5) = \dot{m} c_p (T_2 - T_1) \\
 P_R &= k_{cont} (T_4 - T_6) = \dot{m} c_p (T_3 - T_2) \\
 T_2 &= T_5 - (T_5 - T_1) \cdot e^{-a} \\
 T_3 &= T_6 - (T_6 - T_2) \cdot e^{-a} \\
 a &= \frac{S_{exch} \cdot h_{conv}}{\dot{m} \cdot c_p}
 \end{aligned}$$

Where:

$P_L$  = Power going to the air inlet channel (left in the figure);

$P_R$  = Power going to the right;

$T_i....(i = 1.....6)$  are the problem unknowns, and

$h_{conv}$  = convection heat exchange coefficient ( $\approx 40 \text{ W/m}^2 \text{ K}$ );

$S_{exch}$  = heat exchange area of the fins ( $1.09 \text{ m}^2$ );

$c_p$  = specific heat at constant pressure ( $1007 \text{ KJ/Kg}^\circ\text{C}$ );

$k_{cont}$  = conductance between ACOP chassis and fins block ( $14 \text{ W/K}$ ).

The solution of the equation system tells us that nearly 80% of the thermal load dissipates at the cold side of the fin channels.

80% and 20% respectively of the thermal load will be assumed to be allocated on the slots of the cold side and the hot side respectively. This case is denoted as case 3. The sketch of the thermal load condition and the direction of heat flux is depicted in *Figure 6*.

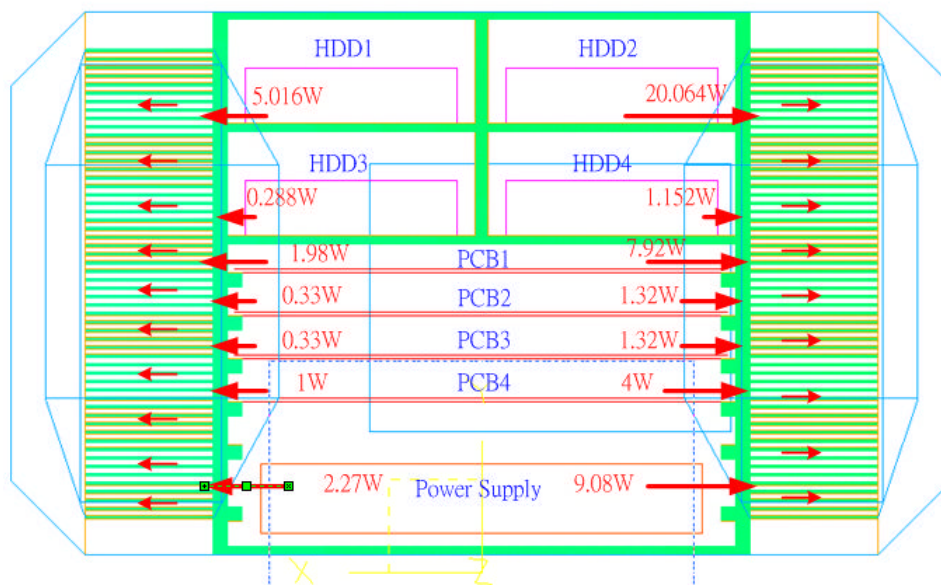



Figure 6: The allocation of ACOP thermal load for case 3 and the sketch of the heat transfer direction

The inlet cooling air conditions and front-panel convection coefficient of ACOP for thermal analysis are listed in *Table 3*.

According to the applicable document [1], the front panel temperature cannot exceed  $49^\circ\text{C}$  for crew contact.

Table 3. Inlet cooling air conditions and front-panel natural convection coefficient			
Inlet air pressure	Inlet air temperature	Inlet air flow rate	Value of h of front panel to ISS cabin
10.2 psia	30 °C	12 cfm	0.965 W/m <sup>2</sup> °C

Table 3: Inlet cooling air conditions and front-panel convection coefficient

 CARLO GAVAZZI SPACE SpA	<h1 style="text-align: center;">ACOP</h1>		Doc N°: <b>ACP-RP-CGS-006</b>
	THERMAL ANALYSIS AND DESIGN REPORT		Issue : <b>1</b> Date: <b>Jan. 2005</b>
		Page <b>17</b> of <b>30</b>	

## 7. MODEL DESCRIPTION AND THERMAL ANALYSIS

### 7.1 THERMAL AND FLUIDIC MODEL DESCRIPTION

For the complicated domain with a coupling of heat transfer and flow dynamics, the computation tool should be dedicated to a flexible and efficiency analysed code in order to obtain the prediction results in a short time. Here "I-DEAS+TMG+ESC" code is applied to solve the computation task. See the reference document [9]. According to the code, the solid and the fluid domain are meshed and the meshes are solved by finite difference method.

The analysed domain is meshed into 224716 elements by the mapped method. For the solid and the fluid, 67,045 hexahedral elements and 157,671 trihedral elements are meshed respectively.

Based on the electrical analogy, thermal model of the solid domain is established to construct a resistance-capacitance thermal network. A hybrid approach is developed in the code by utilizing the element based finite difference method to simulate conduction and surface convection.

The thermal code is coupled with the element based finite volume method flow solver.

Although the Reynolds number of the fin channel flow is calculated to be around 142 to show most regions of the channels belong to a laminar flow, the inlet and the outlet of the channels give the characteristic of turbulence flow due to the flow entry effect. In the laminar flow regions, the turbulence effect will decay to be negligible. Thus, most of the flow regions demonstrate the characteristics of a laminar zone.

Therefore, the laminar flow model for calculation the wall friction and the local heat transfer coefficient is selected in the code.

The distance of two adjacent fins in the channel is 2.5 mm make the smallest size of the meshed elements be 1.25 mm. The Reynolds Number of the inlet duct is calculated to be 2242, close to the critical value (2300). Thus, if the length of the inlet duct and the outlet duct is long enough and the surface is rough, the fully developed flow in the duct will belong to a transient flow swapping between a laminar flow and a turbulent flow. According to the descriptions of the reference document [11], the duct flow should belong to a laminar flow. The duct length is 242 mm. This length is shorter than the length around 500 mm needed for the flow to become fully developed. The flow in the inlet and in the outlet duct belongs to an entry region.

Two approaches of computation in the thermal and fluidic model of ACOP have been performed in order to allow a cross check of the results.

First, the heat transfer coefficient between the cooling air and the solid domain of ACOP is given by hand calculation via the semi-empirical correlation for the fin channel and the ducts.

The second approach is to utilize the laminar flow model on the entire ACOP thermal-fluidic flow field and to carry out the calculation of the ACOP temperature profile, including the structure (aluminium alloy 7075-T7351) and the cooling air.


The thermal conductivity of alloy aluminium 7075-T7351 is adopted as a constant value 151 W/m°C.

#### 7.1.1 INLET AND OUTLET DUCTS, FRONT PANEL

The methodology of the first approach (hand calculation) is described hereafter.

A semi-empirical correlation of Nusselt number in the reference document [13] for a laminar flow in a circular tube has been evaluated.

$$\overline{Nu} = Nu_{\infty} + \frac{K_1 \cdot (\text{Re} \cdot \text{Pr} \cdot D_e / x)}{1 + K_2 \cdot (\text{Re} \cdot \text{Pr} \cdot D_e / x)^n} \quad (1)$$

 CARLO GAVAZZI SPACE SpA	<h1 style="text-align: center;">ACOP</h1>	Doc N°: <b>ACP-RP-CGS-006</b> Issue : <b>1</b> Date: <b>Jan. 2005</b> Page <b>18</b> of <b>30</b>
	THERMAL ANALYSIS AND DESIGN REPORT	

Where  $\overline{Nu}$  is the mean Nusselt number,  $Nu_{\infty}$  is the Nusselt number of the fully developed region,  $D_e$  is the effective tube diameter,  $Re$  is the Reynolds number referred to this diameter,  $Pr$  is the Prandtl number, and  $x$  is the tube length, and  $K_1$ ,  $K_2$ , and  $n$  are semi-empirical constants. By using the given constant  $K_1=0.104$ ,  $K_2=0.016$ , and  $n=0.8$  and the cooling air thermal properties to calculate the value of  $Re$  is around 1,750 at the end of the inlet duct. Thus, the mean value of  $\overline{Nu}$  is calculated to be around 19. However, the aspect ratio of the duct cross-section is to be 4 at the end of the ducts needs a modification on the mean value of  $\overline{Nu}$ . The modified mean value of  $\overline{Nu}$  is estimated to be 23. Therefore, the mean value of the heat transfer coefficient  $h$  is evaluated to be  $6.4 \text{ W/m}^2\text{°C}$  for the ducts.

In the second case (CFD simulation) both the thermal and momentum wall functions are used to calculate the heat transfer coefficient for the solid surface and the cooling air, described by the reference document [9].

$$h_w = \frac{rC_p u^*}{T^+}, \quad h_c = \Theta_y \cdot \Theta_r \cdot h_w, \quad T^+ = (T_w - T)/T^* \quad (2)$$

Where  $h_w$  is the heat transfer coefficient calculated via the thermal wall function of the reference document [10],  $u^*$  is the friction velocity,  $T^+$  is the dimensionless temperature of the fluid,  $\Theta_y$  is a mesh correction factor,  $\Theta_r$  is a roughness factor and  $h_c$  is the convective heat transfer coefficient,  $T_w$  is the wall temperature,  $T$  is the fluid temperature, and  $T^*$  is the characteristic temperature.

With the CFD simulations the calculated results show that the  $h$  mean value is around  $10 \text{ W/m}^2\text{°C}$  for the ducts (to be compared with  $6.4 \text{ W/m}^2\text{°C}$  above calculated) and is around  $8 \text{ W/m}^2\text{°C}$  for the front panel.

The mean value of  $h = 10 \text{ W/m}^2\text{°C}$  calculated from the CFD can be explained considering the enhancing effect of heat transfer rate due to the gradual change of the duct flow cross-section, thus the two values,  $10 \text{ W/m}^2\text{°C}$  and  $8 \text{ W/m}^2\text{°C}$ , are adopted as acceptable.

Moreover it must be pointed out that, since inlet and the outlet duct have a total area around  $0.121 \text{ m}^2$ , they play a minor role to cool down the ACOP compared to the fin channels, each with a total area around  $1.09 \text{ m}^2$ , ten times larger.

### 7.1.2 FINNED CHANNELS

Most of the power dissipation of ACOP boards is directly conducted to the fins and then to the ducts. According to the semi-empirical correlation of the Nusselt number for the channel flow (that plays the key role in the heat transfer), the  $h$  value of the fin channel is calculated to be  $40.3 \text{ W/m}^2\text{°C}$  with an aspect ratio of 24 for the channel cross section.

For the CFD laminar flow model the heat transfer coefficient is around  $42.1 \text{ W/m}^2\text{°C}$ , as compared to the semi-empirical value  $40.3 \text{ W/m}^2\text{°C}$  with an uncertainty of around 4.5%.

## 7.2 THERMAL CASES

Considering the laminar flow model in the entire flow established in version 8.0 of ESC and the applied mean value of  $h$  via the semi-empirical correlations, and the differently allocated thermal load due to different locations of the two working HDD's, three cases will be carried out in this report. For case 1, the two working HDD's are put on the top of ACOP; for case 2, the two working HDD's are installed on the hot side of ACOP. Both of them are solved with the laminar flow model. Case 3 denotes the case with 80% of the thermal load allocated to the air inlet side and 20% to the air outlet side. The summary of these five cases is given in *Table 4*.

The inlet cooling air temperature is fixed to be  $30 \text{ °C}$  in all the cases.

One operation mode only is considered for ACOP.

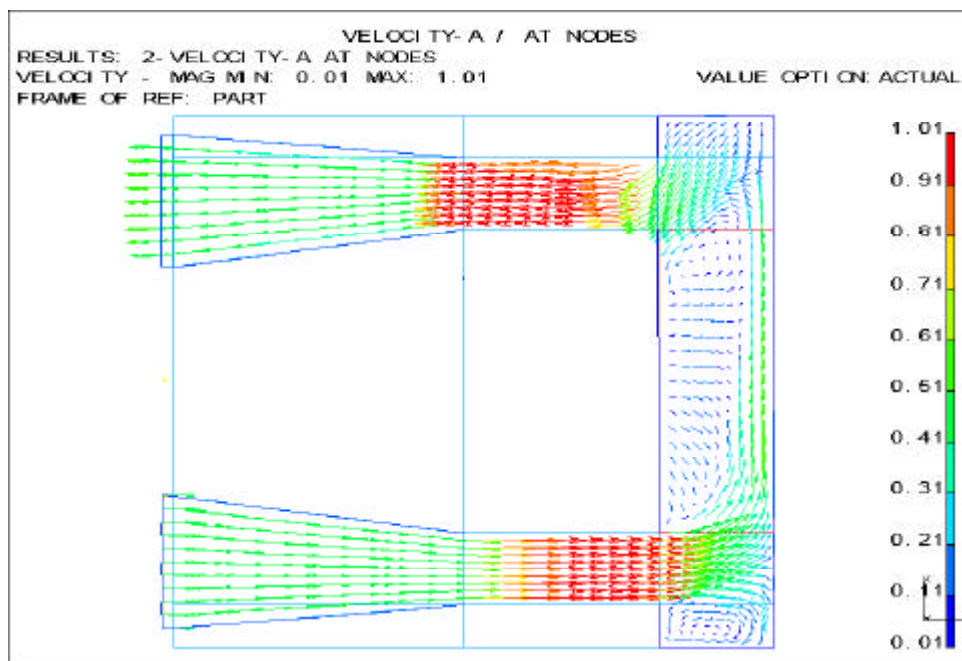
	Thermal Load	Hottest Location	Max. Temperature (°C)
Case 1	See Figure 3	Top centre of chassis	44.1
Case 2	See Figure 4	Top centre of chassis	45.2
Case 3	See Figure 5	Outlet of hot fin channels	43.7

Table 4: Predicted maximum Temperature for the analysed cases

## 8. ANALYSIS RESULTS

The cooling air velocity field at the locker mid-height is shown in *Figure 7*. The predicted results show that the maximum velocity at the centre of the fin channels is around 1.0 m/sec.

The entrance effect of the fin channels on the velocity variation is also predicted in the model. The variation of the air velocity along flow direction due to the change of the cross section area of the ducts is well seen. The velocity of the air flow varies smoothly in the inlet duct and in the inlet fin channel. However, at the outlet of the fin channels at the cold side produces recirculation due to the expansion. Theoretically both the flow velocity and the Reynolds number are low enough to produce a laminar flow in the fluid domain. However, at the channel outlet the eddy will yield a turbulence effect to enhance the heat transfer rate. Simultaneously the pressure loss due to the turbulent eddies also happens in this region. The pressure loss will be much higher than the wall friction loss under the laminar flow. At both ends of the front panel chamber, flow impingement phenomena occur resulting into enhanced heat transfer and larger pressure losses.



*Figure 7: Predicted velocity along the middle cross section of ACOP with a flow rate of 12 cfm*

The calculated heat transfer coefficient  $h_c$  is 42.1 W/m<sup>2</sup>°C at the central part of the fins due to a thin gap of 2.5 mm between the adjacent fins. See *Figure 8*.

Because the laminar flow model is applied in calculation, the transient entry effect is neglected to result into a constant calculated value of the heat transfer coefficient  $h$  as 42.1 W/m<sup>2</sup>°C.

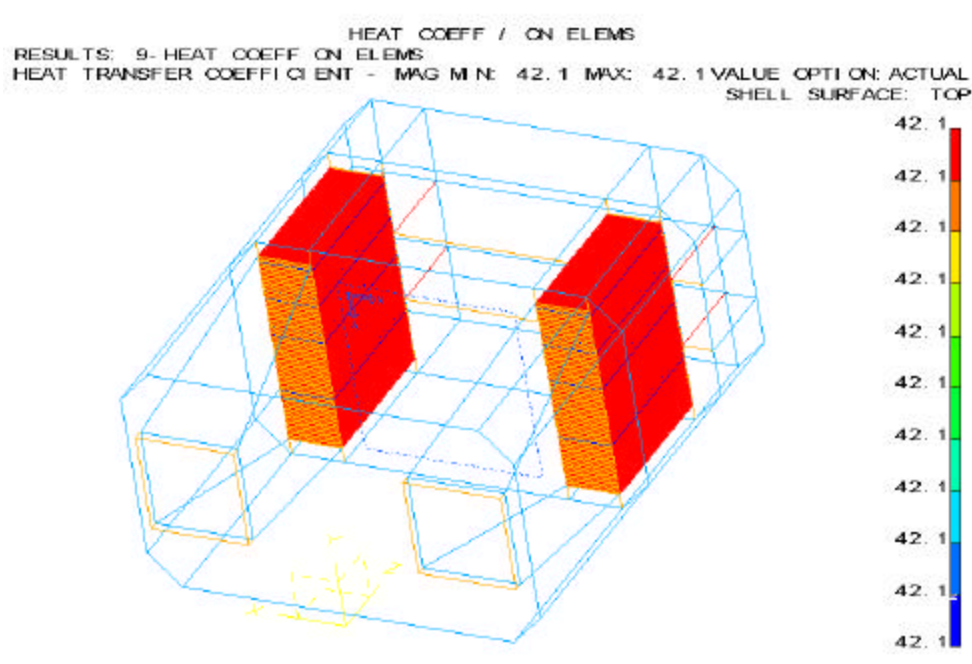


*Figure 8: Predicted heat transfer coefficient in the fin channels via the laminar flow model*

With a mean value of  $h_c$  around 42.1 W/m<sup>2</sup>°C and the large value of the total fin area, 2.18 m<sup>2</sup>, the predicted chassis/fin temperature is around 35.7 °C at the inlet region of the fin channels at the cold side, and is around 43.7 °C at the outlet region of the fin channels at the hot side.

The maximum temperature occurs at the central chassis for mounting the HDD's to be around 44.1 °C, as shown in *Figure 9*. The predicted temperature distribution of the fin channel of the hot side is very uniform, resulting from the high thermal conductivity of the channels.

Air cooling is not introduced into the central chassis of top ACOP. However, the thermal conductivity of chassis is high enough to conduct the power dissipation of HDD's effectively to the remaining regions of the chassis, leading to a significant reduction of the working temperature.

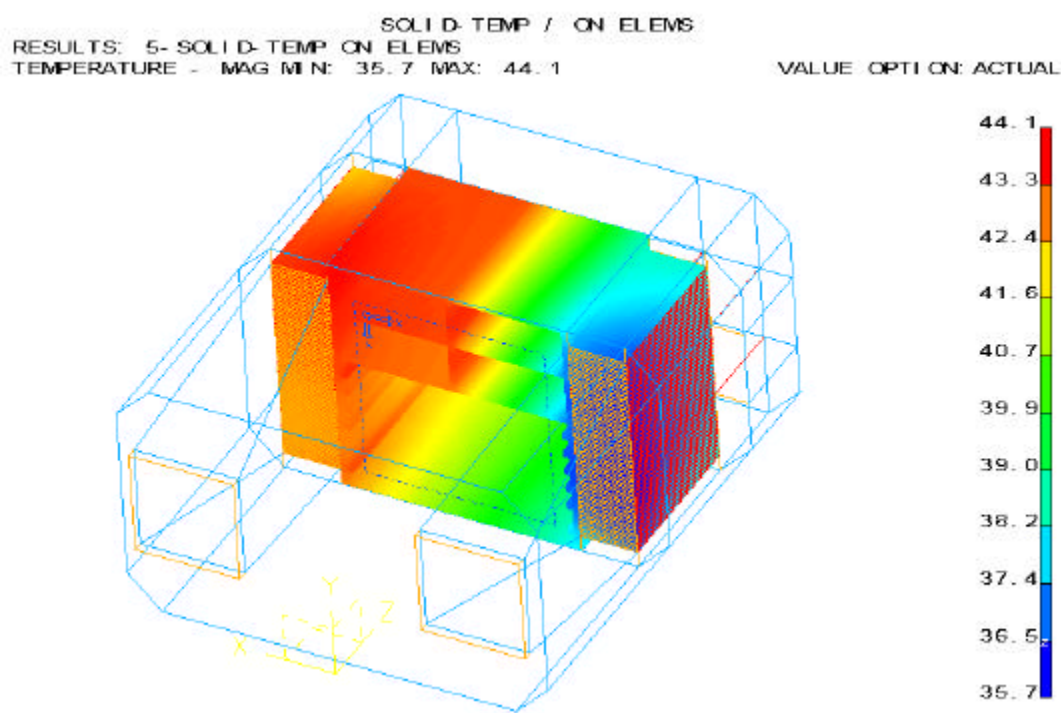


*Figure 9: Predicted temperature profile of the fin channels and chassis for case 1*

Figure 10 shows the predicted temperature profile of the front panel for case 1. Although the power dissipation of the LCD monitor is provided by 6.3 W, the heat is transferred to the adjacent regions of the ACOP enclosure effectively, resulting into a maximum temperature of around 41.4 °C at the centre of the LCD monitor.

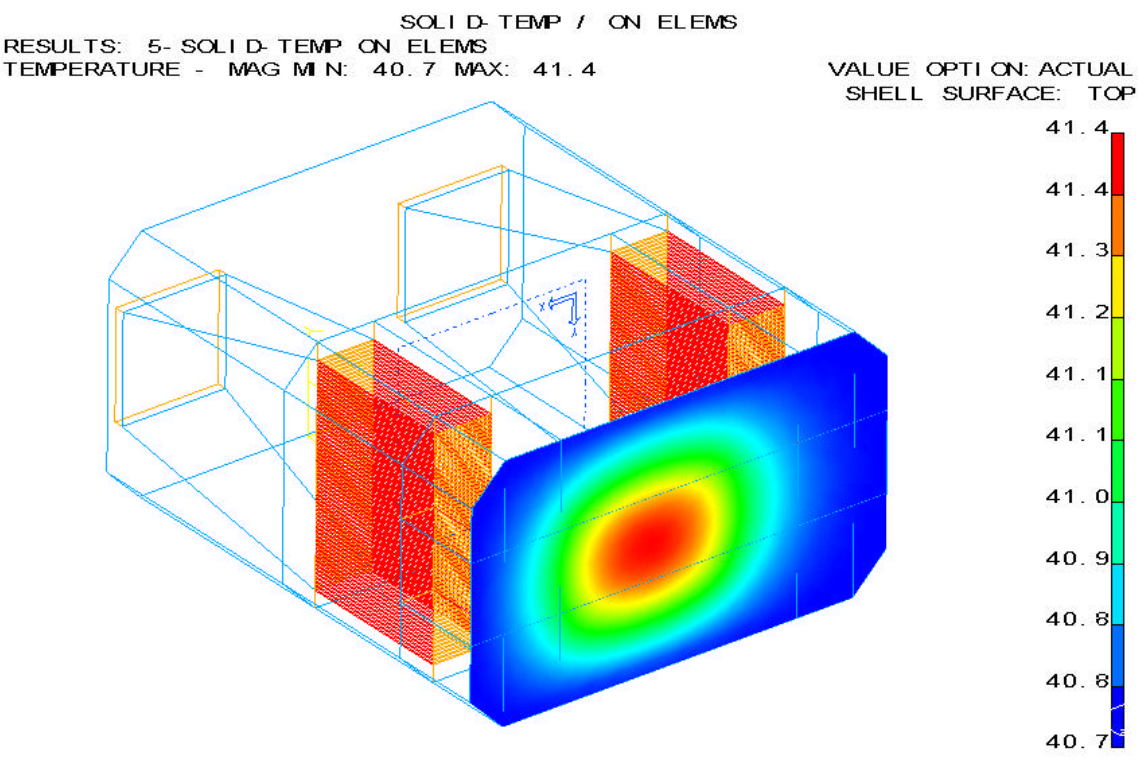


Figure 10: Predicted temperature profile of the front panel for case 1

Figure 11 shows the predicted temperature profile of the cooling air. The cooling air is gradually heated in ACOP from the inlet to the outlet. The air temperature increases by around 10 °C to be 40 °C at the outlet of the channels at the cold side. In the front panel chamber, the air is heated by more than 1 °C. Finally in the channels on the hot side, the air temperature is high as compared to the ACOP inlet condition, and can take away a smaller portion of the total power dissipation, with a lower increase of the air temperature to be around 43 °C at the outlet of the channels on the hot side.

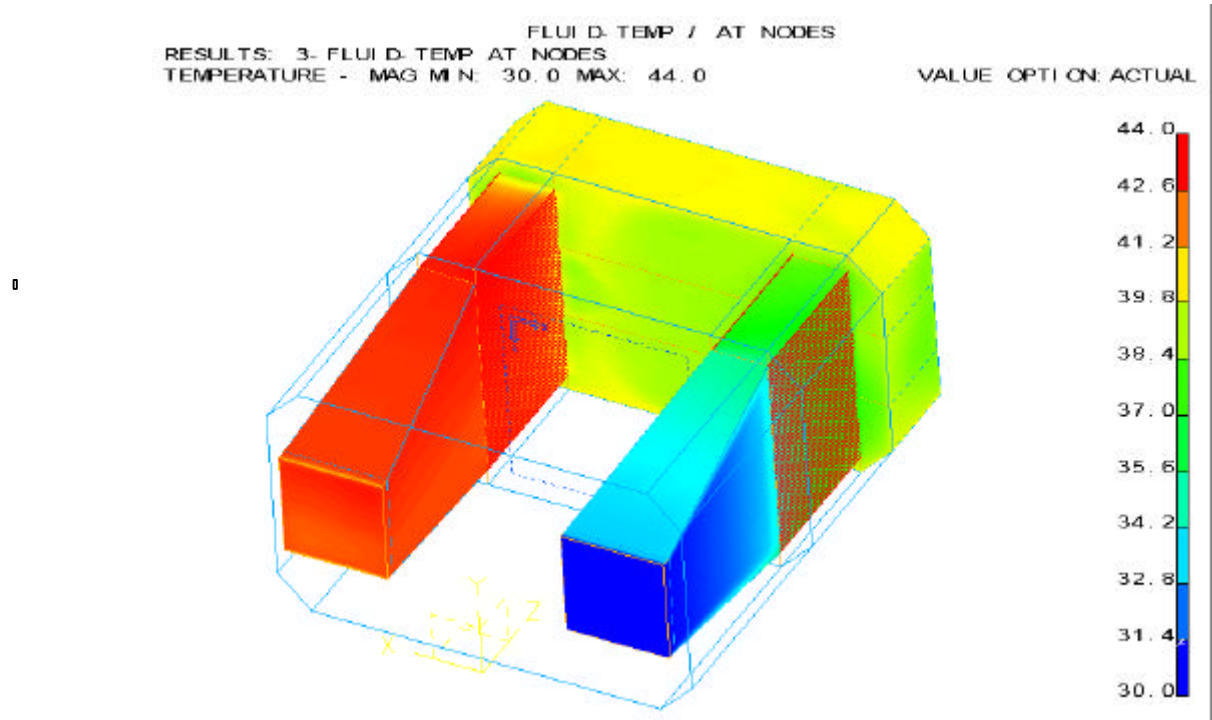


Figure 11: Predicted temperature profile of the cooling air for case 1

Figures 12 and 13 show the predicted temperature profile of the cooling air at the mid height plane, and the mid section. The thermal load is larger at the top of ACOP than the bottom, and therefore the temperature of the air is higher in the top regions.

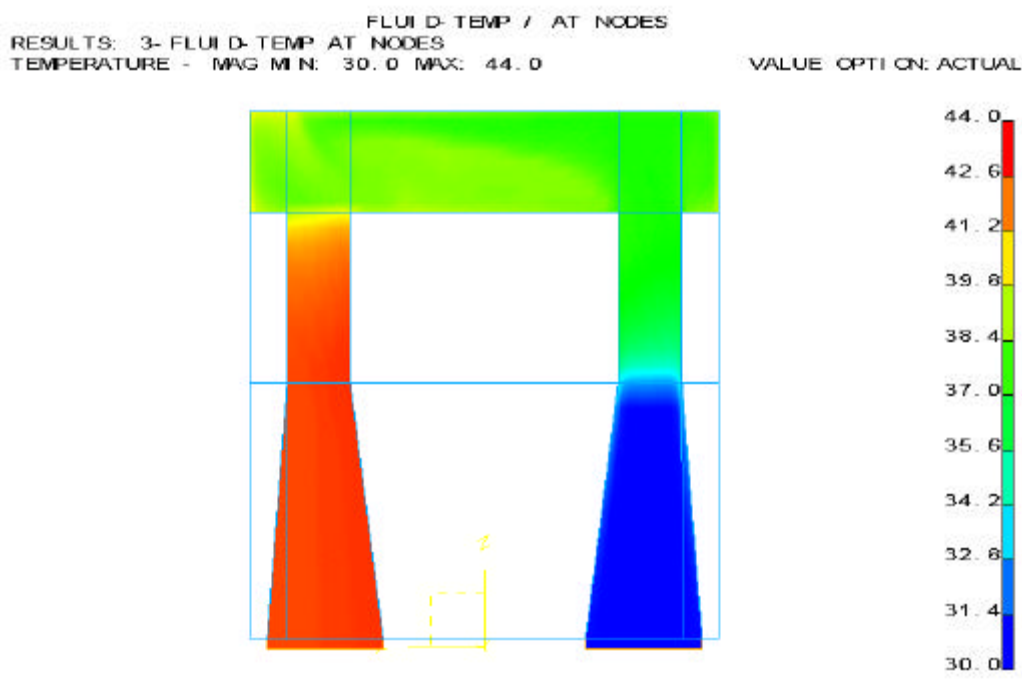


Figure 12: Predicted temperature profile of the cooling air at the central section of ACOP for case 1

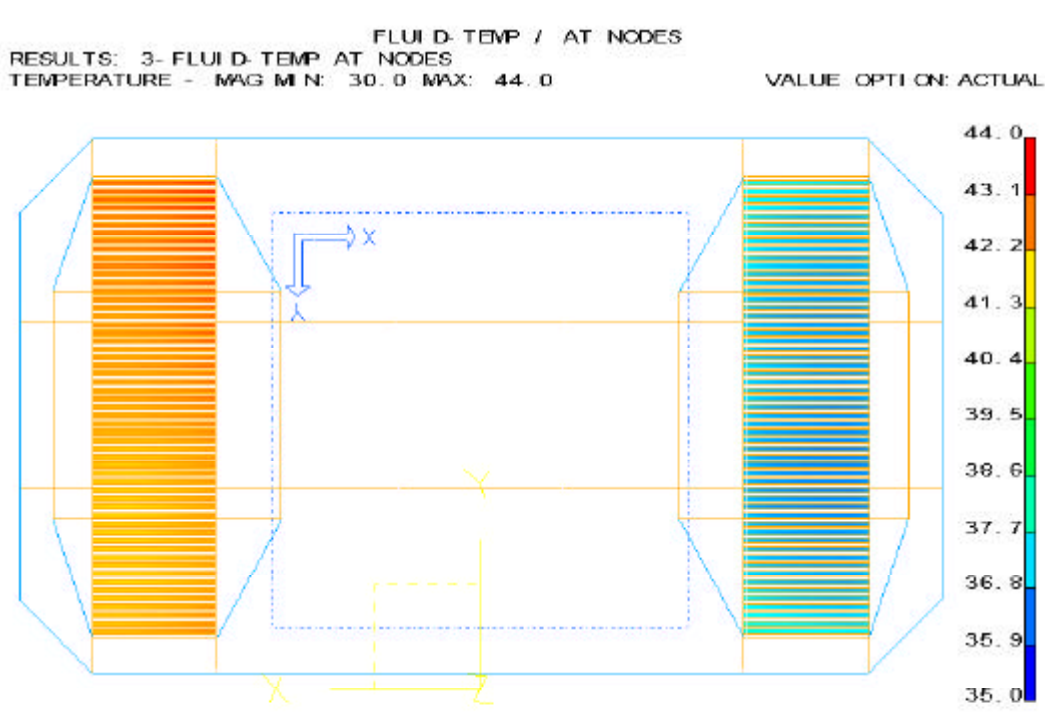


Figure 13: Temperature profile of air in the fin channels at the central cross section for case 1

Figure 14 shows the predicted ACOP temperature profile of the channels and the chassis for case 2. As the thermal load of the two working HDD's is allocated evenly on the top slots, the central top chassis needs to spread 12.54 W to the fin channels. See Figures 3 and 4. It means that the thermal load density of the HDD's for case 2 is two times of case 1 on the slot of the central top chassis. This leads to an increase temperature by near 1 °C for case 2 as compared to case 1, at the central top chassis. The predicted temperature reaches 45.2 °C. The cooling air temperature profile is similar to that of case 1, not shown here. Although the two working HDD's are installed at different locations of ACOP, the working temperature of the chassis varies less than 1.5 °C as a comparison of the temperature difference of case 1 and case 2.

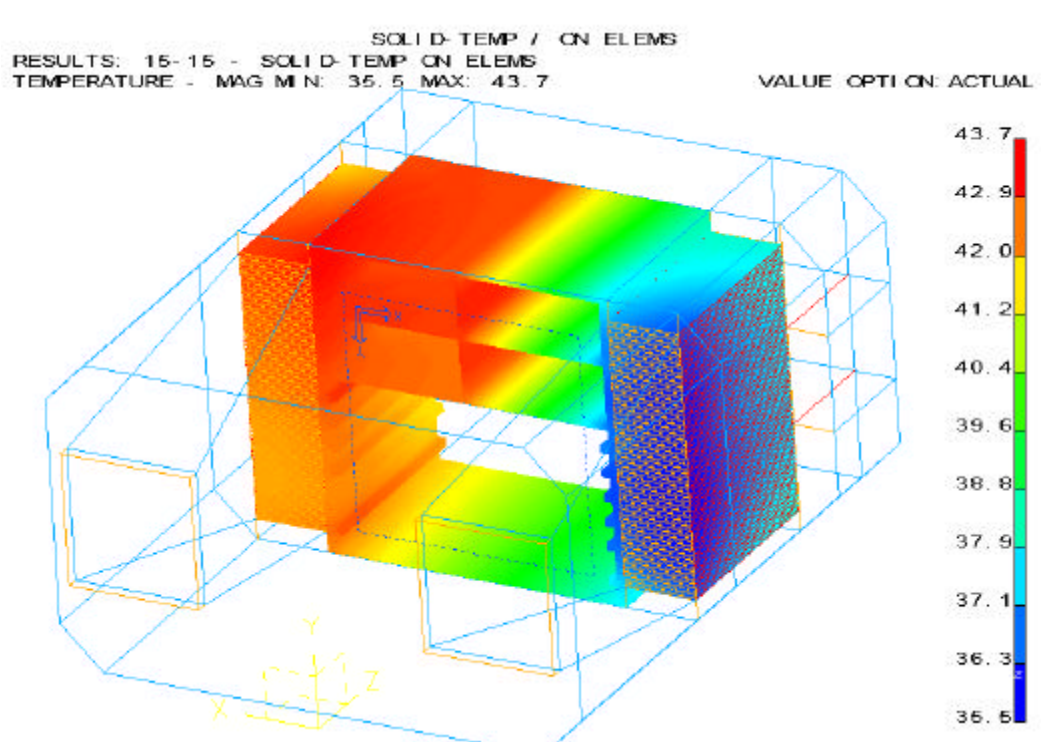
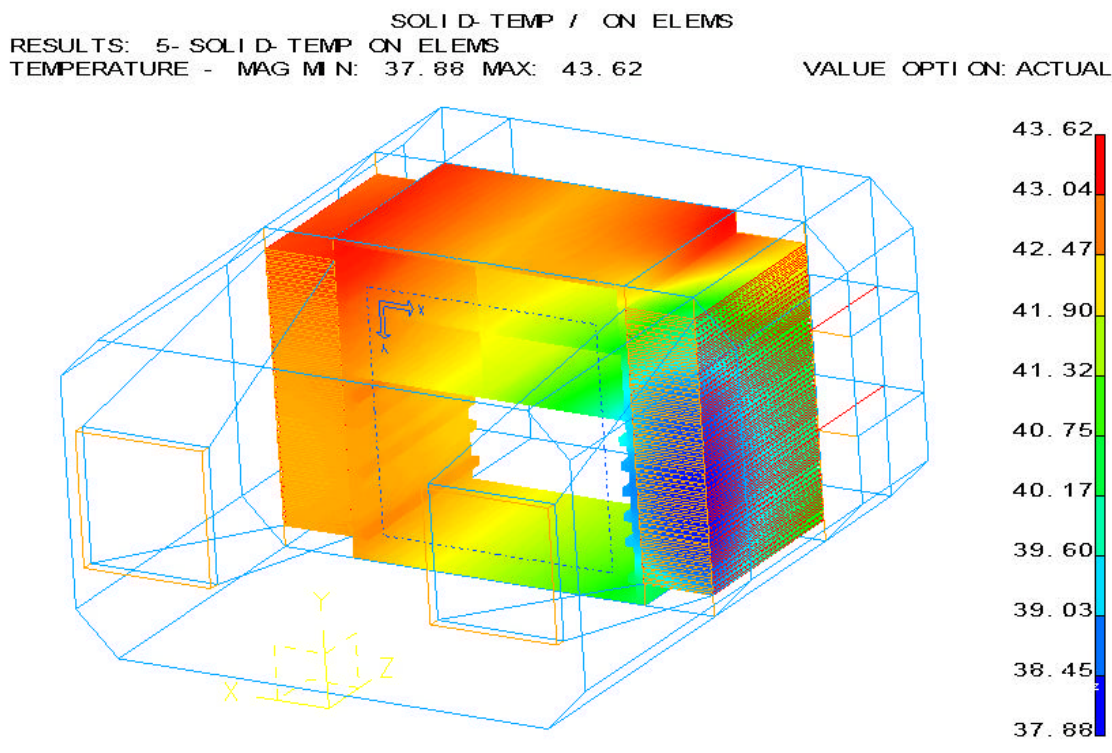


Figure 14: Predicted temperature profile of the fin channels and chassis for case 2

The predicted temperature distribution of ACOP chassis and fin channels for case 3 is shown as *Figure 15*. The 80% of the thermal load is allocated on the slots of the cold side, resulting into that the chassis temperature of the cold fin channel is higher than cases 1 and 2 for around 2 °C. The hot spot of ACOP chassis changes to the outlet of the fin channels at the hot side from the centre of ACOP chassis.




*Figure 15: Predicted temperature profile of the fin channels and chassis for case 3*

*Table 4* provides the predicted maximum temperature for cases 1 to 3 respectively. Although by applying different allocations of the thermal load and different models for the given boundary conditions of the chassis, the temperature difference is around the order of 1-2 °C.

Under the pressure value 15.2 psia of the supplied cooling air, the outlet air temperature will decrease to be around 39.4 °C.

If the air flow rate increases to be the maximum limited value 18 cfm, the heat transfer coefficient is assumed to enhance insignificantly in ACOP. Thus, under the same pressure 10.2 psia and the same inlet temperature 30 °C, the outlet air temperature will decrease to be 39.3 °C. Similarly, the chassis and the fin temperature will be decreased by around 4.7 °C while the heat transfer coefficient increases insignificantly.

The calculated results show that the front panel dissipates around 1.1~1.2 W to the ISS cabin environment for these cases.

 CARLO GAVAZZI SPACE SpA	<h1 style="text-align: center;">ACOP</h1>	Doc N°: <b>ACP-RP-CGS-006</b> Issue : <b>1</b> Date: <b>Jan. 2005</b>
	THERMAL ANALYSIS AND DESIGN REPORT	Page <b>28</b> of <b>30</b>

## 8.1 PRESSURE LOSS

The system pressure loss can be roughly calculated by the semi-empirical equations of pressure loss due to the wall friction of the fluid, and the inlet and the outlet of conducts and the fin channels due to an abrupt expansion or an abrupt contraction of the fluid.

$$\Delta P = f \cdot \frac{L}{D_e} \cdot \frac{1}{2} \cdot \rho \cdot V_m^2 \quad \text{For duct and channel flow} \quad (3)$$

$$\Delta P_j = C_f \cdot \frac{1}{2} \cdot \rho \cdot V_m^2 \quad \text{For joints} \quad (4)$$

Where  $\Delta P$  is the pressure loss due to the wall friction,  $f$  is the friction coefficient,  $L$  is the length of the duct or the channel,  $D_e$  is the effective diameter of the channel or the duct,  $V_m$  is the mean bulk velocity of the channel or the duct,  $\Delta P_j$  is the pressure loss due to a flow expansion or contraction at the joint connecting different flow parts and  $C_f$  is the coefficient of pressure loss due to a flow expansion or contraction at the joint.

The entry transition, and the recirculation due to the outlet expansion or the inlet contraction and the impingement effect could be ignored due to the restriction of the laminar flow model.

Because the screens have an open area ratio of 0.602 and with a small effective diameter of the wires and holes, the friction coefficient is conservatively calculated to be close to 2. The total pressure loss of the cooling air through the two screens on the inlet and outlet is calculated to be 0.97 Pa.

For the fin channels, the ratio of the length to the effective diameter is calculated to be around 33 times of the effective diameter. According to the data of the reference document [11], the entry length of the fin channel is calculated to be 4 times of the space between two adjacent fins (for the flow rate 12 cfm). The entry length occupies about 6% of the total length. The assumption of the flow in the fin channel belonging to a fully developed laminar flow is used to calculate the pressure loss due to the wall friction of the cooling air. The entry length is calculated via the semi-empirical equation,


$$\frac{x_{fd}}{d_s} \approx 0.05 \cdot \text{Re}_s \quad (5)$$

Where  $x_{fd}$  is the length needed for the flow becoming fully developed,  $d_s$  is the space between two adjacent fins,  $\text{Re}_s$  is the Reynolds number based on the value of  $d_s$ .

The original semi-empirical equation is developed for a circular tube, and here, we applied the equation on the fin channel based on the value of  $d_s$ , replacing the effective diameter. By the analogy of the boundary thickness of the tube and the fin channels, equation (5) should be applied based on the value of  $d_s$ .

According to the applicable document [14], the developing channel flow effect on the pressure loss can be modified by a constant coefficient  $K_\infty$  and the correlation equation (4) is re-written as

$$\Delta P = \frac{1}{2} \cdot \left( f \cdot \frac{L}{D_e} + K_\infty \right) \cdot \rho \cdot V_m^2 \quad (6)$$

  CARLO GAVAZZI SPACE SpA	<h1>ACOP</h1>	Doc N°: <b>ACP-RP-CGS-006</b>
	THERMAL ANALYSIS AND DESIGN REPORT	Issue : <b>1</b> Date: <b>Jan. 2005</b>
		Page <b>29</b> of <b>30</b>

Here, the aspect ratio of the fin channel flow as 24 will provide the values of  $f$  and  $K_{\infty}$  by the followings,

$$fR_e = 93,$$

$$K_{\infty} = 0.72 \quad (7)$$

Table 5 shows the pressure loss of the fin channel flow at one side calculated via the above equations (6) and (7) with different flow rates and air pressure. It seems that the entrance effect and the air pressure effect on the pressure loss of the 162 mm fin channel is much less than that of the flow rate.


Pressure	10.2psi						15.2psi					
	$V_m$ (m/s)	$\rho$ (kg/m <sup>3</sup> )	$D_e$ (m)	Re	$f$	$\Delta P$ (Pa)	$V_m$ (m/s)	$\rho$ (kg/m <sup>3</sup> )	$D_e$ (m)	Re	$f$	$\Delta P$ (Pa)
<b>Flow rate</b>												
<b>12cfm</b>	<b>0.686</b>	<b>0.798</b>	<b>0.0048</b>	<b>142</b>	<b>0.655</b>	<b>4.28</b>	<b>0.686</b>	<b>1.189</b>	<b>0.0048</b>	<b>211.6</b>	<b>0.44</b>	<b>4.35</b>
<b>15cfm</b>	<b>0.8575</b>	<b>0.798</b>	<b>0.0048</b>	<b>177</b>	<b>0.524</b>	<b>5.4</b>	<b>0.8575</b>	<b>1.189</b>	<b>0.0048</b>	<b>264</b>	<b>0.352</b>	<b>5.5</b>
<b>18cfm</b>	<b>1.029</b>	<b>0.798</b>	<b>0.0048</b>	<b>213</b>	<b>0.4366</b>	<b>6.53</b>	<b>1.029</b>	<b>1.189</b>	<b>0.0048</b>	<b>317</b>	<b>0.293</b>	<b>6.67</b>

Table 5: Fin channel pressure loss of one side with different flow rates and pressures of cooling air via the semi-empirical correlations

The coefficient of the pressure loss due to an expansion or a contraction flow at the joints of the fin channel with the ducts or the chamber is assumed to be unity if the leading edges of the fins are made round and smooth at the joints. The flow turn of the air leaving from or entering into the fin channels also produces a pressure loss. The value of  $C_f$  is also treated as unity.

Thus, the pressure loss includes the screens on the inlet and the outlet ports connecting the ACOP and the EXPRESS rack locker ducted cooling air to be 0.97 Pa, friction on the inlet and the outlet ducts for the fin channels to be around 0.1 Pa, an expansion and contraction of the inlet region and the outlet region of the fin channels to the ducts and the panel chamber to be 0.75 Pa, friction on the fin channel wall of two sides to be 8.70 Pa, the flow turn of the cooling air in the front panel chamber to be 0.375 Pa, and friction on the panel chamber to be 0.1 Pa. Thus, the total system pressure loss is calculated to be around 10.995 Pa for the flow rate 12 cfm and the inlet air pressure 10.2 psia.

For the worst case of the system pressure loss, the flow rate 18cfm and the air pressure 15.2 psia, the loss of two screens is calculated as 3.252 Pa, friction on the inlet and the outlet ducts as 0.15 Pa, the chamber as 0.1 Pa, the joint loss of the fin channels with the ducts and the chamber as 2.515 Pa, the turn flow in the front chamber as 1.258 Pa, and friction loss on the fin channels of two sides as 13.34 Pa. Thus, the total system pressure under the worst case is estimated to be 20.61 Pa.

 CARLO GAVAZZI SPACE SpA	<h1>ACOP</h1>		Doc N°: <b>ACP-RP-CGS-006</b>
	THERMAL ANALYSIS AND DESIGN REPORT		Issue : <b>1</b> Date: <b>Jan. 2005</b>
		Page <b>30</b> of <b>30</b>	

## 9. CONCLUSIONS

The introduction of fin channels extruded out from ACOP chassis can provide two enhancing effects on the heat transfer rate from chassis to the cooling air. The apparently significant effect is due to a large increase of the area value for forced convection of the cooling air. The other enhancing effect of heat transfer results from a reduction of the channel gap, leading to an increase of the heat transfer coefficient. Both effects make the effective thermal resistance between the cooling air and ACOP be low enough, leading to a predicted maximum increase temperature by around 15 °C at the chassis centre for mounting the HDD's based on the fluid model developed in the ESC module.

The outlet temperature of the cooling air is calculated to be around 44 °C less than the requirements of the exhaust temperature 49 °C in the applicable reference [1]. This is compliant to the system requirements.

The maximum front panel temperature is predicted to be 41.4 °C less than the maximum temperature limit of 49 °C.

The predicted heat transfer coefficient 42.1 W/m<sup>2</sup>°C of the cooling air in the fin channels via the laminar flow model is slightly larger than the calculated value 40.3 W/m<sup>2</sup>°C by the semi-empirical correlation. Different allocations of the thermal loads are considered from the boards and the HDD's. The predicted results show that the temperature discrepancy of the chassis for the maximum value of the three different cases is around 1-2 °C.

For the flow rate of the supplied air 12 cfm, the pressure 10.2 psia, and temperature 30 °C, the calculated result 10.865 Pa via the semi-empirical correlations. If the flow rate increases to the maximum value of 18 cfm and the air pressure to be 15.2 psia, the maximum calculated system pressure loss is 20.61 Pa.

Under the worst case with the minimum air flow rate 12 cfm and with the maximum supplied air temperature 30 °C, the calculated maximum chassis temperature around 45 °C is below the required temperature of 50 °C.

Thus, the currently thermal management design is appropriate for ACOP to dissipate the power consumption effectively.